Ocean-sea ice processes and their role on multi-month predictability of Antarctic sea ice

Stephy Libera[1,2], Will Hobbs[3,2], Andreas Klocker[4], Amelie Meyer[1,2], Richard Matear[5]

[1] Institute for Marine and Antarctic Studies, University of Tasmania, Hobart, Tasmania.
[2] Australian Research Council Centre of Excellence for Climate Extremes,
[3] Australian Antarctic Program Partnership, Institute for Marine and Antarctic Studies, University of Tasmania, Hobart, Tasmania.
[4] Department of Geosciences, University of Oslo, Oslo, Norway.
[5] CSIRO Oceans and Atmosphere, Hobart, Tasmania.

Corresponding author: Stephy Libera (stephy.libera@utas.edu.au)

†

Key Points:

- Antarctic sea ice predictability is strongly determined by the temperature and salinity profiles of the underlying upper ocean water column
- Every winter, the timing of the loss of sea ice predictability is defined by when deep water is entrained into the mixed layer
- Sea ice predictability depends not only on the depth of the Winter Water layer, but also on how strongly stratified its base is

Abstract

Antarctic sea ice is a critical component of the climate system and a vital habitat for Southern Ocean ecosystems. Understanding the underlying physical processes and improving Antarctic sea ice predictability is of broad interest. Using model data, we investigate sea ice and upper ocean predictability at interannual timescales in the Weddell Sea region. We find that oceanic predictability is largely confined to the Winter Water layer and responds to seasonal modifications of the water column, mainly driven by sea ice processes. Predictability depends not only on the depth of the Winter Water layer, but also on how strongly stratified its base is. Predictability is lost when warm Circumpolar Deep Water with no sea ice-related memory entrains into the mixed layer. We show the strong dependence of sea ice predictability on the local upper ocean vertical structure, which suggests that both are likely to change in a warming climate.

Plain Language summary

Antarctic sea ice affects global climate through its interplay with planetary albedo, atmospheric circulation, thermohaline circulation, ocean productivity, and is also a vital habitat for Southern Ocean ecosystems. Therefore, understanding the drivers and physical processes influencing Antarctic sea ice, and being able to predict Antarctic sea ice, is of broad interest.

We assess the predictability of sea ice and underlying upper ocean in the Weddell Sea region of the Southern Ocean using model data. We find that sea ice processes influence the upper ocean temperature, and these thermal signatures linger in the ocean producing sea ice predictability over multiple months. Here we show the oceanic memory (lingering thermal signature) in the upper ocean is largely found within the Winter Water layer (WW i.e., cold water layer formed during sea ice formation). Oceanic memory and sea ice predictability are suddenly lost when warm deep waters from the ocean interior entrain into the surface mixed layer in mid-winter. This limit to sea ice predictability has not been explored before, and it shows the strong dependency of sea ice predictability in a region to its local vertical structure of oceanic properties and their seasonal evolution. This implies that the spatial variability in sea ice predictability can now be addressed based on local upper ocean vertical structure and sea ice processes. Also, changes to upper ocean properties in a warming climate can likely alter the sea ice predictability patterns in the future.

1 Introduction

The growth and melt of Antarctic sea ice, arguably the strongest seasonal cycle on the planet (Handcock and Raphael, 2020), affects global climate through its interplay with planetary albedo, atmospheric circulation, thermohaline circulation, and ocean productivity (Abernathey et al., 2016; Brandt et al., 2005; Hobbs et al., 2016; Massom and Stammerjohn, 2010; Raphael and Hobbs, 2014). The close interaction of Antarctic sea ice with the ocean and atmosphere has been linked to interannual variability and trends in sea ice (Hobbs et al., 2016; Holland, 2014; Lecomte et al., 2017; Martinson, 1990). Antarctic sea ice predictability studies have identified the strong dependence of sea ice predictability on oceanic processes, pointing towards sea ice-ocean interactions (Holland et al., 2013; Marchi et al., 2019; Ordoñez et al., 2018; Zunz et al., 2015). This study aims to better understand the physical processes in the ocean associated with sea ice predictability.

Sea ice predictability studies are diverse, with predictions ranging from seasonal to decadal timescales, using statistical or dynamical approaches, and based on observations or climate model data. They have a variety of applications ranging from planning operational activities (scientific research, tourism, shipping, fisheries management, and conservation) to evaluating climate projections, and policy decision making (Bushuk et al., 2021; Chen and Yuan, 2004; Guemas et al., 2016; Holland et al., 2013; Juricke et al., 2014; Kearney et al., 2021; Marchi et al., 2020; Marchi et al., 2019; Massonnet et al., 2019; Ordoñez et al., 2018; Yang et al., 2016; Zampieri et al., 2019; Zunz et al., 2015). In this study, we evaluate sea ice and ocean predictability at seasonal to interannual timescale in the Weddell sector (Figure 1a). In the Southern Ocean, the Weddell Sea is one of the dominant regions of sea ice production. Its geographical setting limits dynamical influence from advected oceanic and sea ice properties into this region, making it ideal for studying local ice-ocean interaction.

Previous studies have established the link between the upper ocean heat content (OHC) and sea ice predictability (Holland et al., 2013; Marchi et al., 2019). These studies found that sea ice predictability can persist for some months but is then generally lost during the ice-retreat season before reemerging in the following ice-growth season. Marchi et al. (2019) calculated the predictability of integrated OHC in the upper 100 m and showed strong correspondence between regions of high sea ice predictability and oceanic predictability. When integrating the OHC as done by Marchi et al. (2019), information about the evolution of OHC anomalies in the vertical oceanic layers is lost, this limits our capacity to observe the physical process occurring within the ocean.

In this study, we retain the vertical dimension for oceanic predictability results and compare the evolution of predictability of sea ice and ocean simultaneously. We find the loss of predictability in summer followed by the reemergence of predictability in autumn consistent with Holland et al. (2013) and Marchi et al. (2019). We also find a sudden loss of predictability in mid-winter when warm Circumpolar Deep Water is entrained into the mixed layer, connecting the influence of local vertical ocean structure and sea ice processes. These findings not only give insights into the physical processes in the upper ocean underlying sea ice predictability, but also directs towards hydrographic features that are valuable for understanding the regional differences in Antarctic sea ice trends and variability.

2 Methods

2.1 Data

We use the outputs from a global coupled ocean-sea ice model, the Australian Community Climate and Earth System Simulator (ACCESS-OM2), (Kiss et al., 2020). ACCESS-OM2 is based on the ocean MOM5.1 and ice CICE5.1 models coupled with the OASIS-MCT coupler. The model experiment analyzed in this study was forced using JRA55-do v1.4.0 (Tsujino et al., 2018). The high horizontal resolution of 0.1 ^{o} in ACCESS-OM2-01 produces good representation of Southern Ocean dynamics, and adequate simulations of the Antarctic sea ice extent and concentration: The mean annual cycle of Antarctic sea ice extent from ACCESS-OM2-01 closely matches observations and the historical sea ice trends are also well represented (Kiss et al., 2020).

To calculate the observed sea ice area (SIA) used in this study, we use sea ice concentration (SIC) derived from satellite passive microwave data (a product based on the NASA Goddard-merged parameter in the NOAA/NSIDC Climate Data Record (CDR)) (Meier et al., 2013).

2.2 Correlation Analysis and Statistical methods

In our diagnostic predictability analysis, we calculate the correlation between a given initial month and the twelve future months. We use monthly data from 1985 to 2015. For the sea ice area, we calculate the monthly time series of total SIA in Weddell sector and detrend it by subtracting the linear least-squares fit, then we apply the correlation analysis (hereafter referred to as ‘sea ice predictability’). To evaluate the predictability of the ocean from its initial state, we apply the correlation analysis to the detrended monthly timeseries of conservative temperature (T) vertical profiles in the upper 200 m, by spatial averaging in the Weddell sector (T from initial month correlated with future T at same depth) (hereafter referred as ‘ocean-ocean correlations’). Then using the detrended monthly timeseries of total SIA and T in upper 200 m, we calculate correlations between given initial SIA with future T at depth, to investigate the signature of ice-ocean interactions (hereafter referred to as ‘ice-ocean correlation’). We define statistically significant values as p-values greater than 95% in the two-tailed Student’s T-test.

2.3 Climatology

To understand the general ice and ocean seasonal evolution in the Weddell sector, we create the monthly climatologies of temperature (T) and salinity (S). Further the monthly climatology for the vertical gradient of T (dT/dz), S (dS/dz) and density (dρ/dz) are also created. To discuss the upper ocean processes, we use the mixed layer depth (MLD), here an output from the model, which is defined by an increase in density by 0.03 kgm^{-3} from surface ocean density.

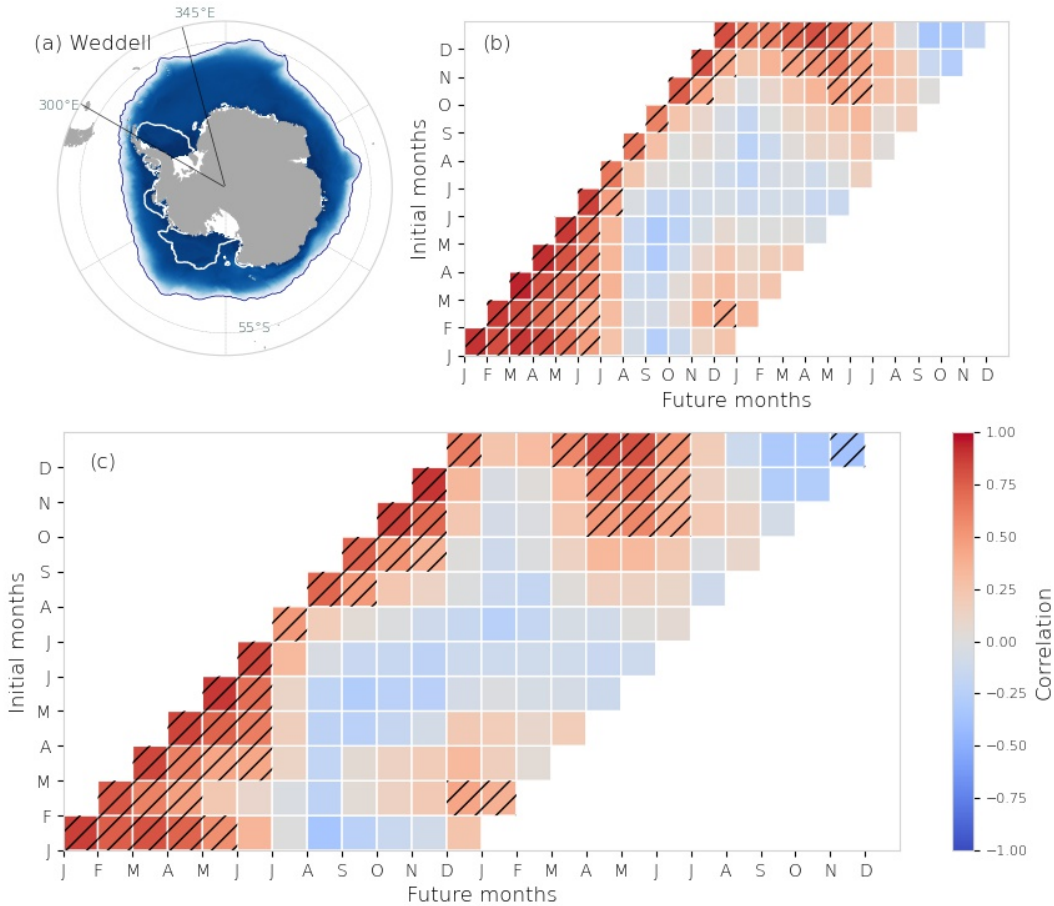

Figure 1: (a) Map defining the Weddell sector in Antarctica along with the model climatological winter maximum (September) of sea ice extent (in shading) and summer minimum (February, white contour). (b) Sea ice predictability: autocorrelation of sea ice area from observation, and (c) Sea ice predictability from model output. In (b) and (c), SIA from initial months (or lead) along y-axis are correlated against the SIA in the future months (or lags) along x-axis and statistically significant values (>95%) are hatched. Summer persistence (*) and spring reemergence (**) patterns are marked in (c).

3. Results

3.1 Sea ice predictability: Summer persistence and spring reemergence

Our analysis of sea ice and ocean predictability is in the forward-looking perspective, that is indicating how a given initial state relates to the future states. Sea ice area predictability results from observations and model data are similar (Figure 1 b, c), and show two predictability patterns: ‘persistence’ from summer initial months with correlations lasting till June, shown by a sustained significant autocorrelation (Figure 1c *); and ‘reemergence’ from spring initial months to the following autumn months (Figure 1c **), shown by the loss of correlation in summer months which ‘reemerges’ in April. These patterns of persistence in summer and reemergence from spring to autumn (hereafter ‘spring reemergence’) were identified in a similar diagnostic study by Ordoñez et al 2018. Prognostic studies have identified the reemergence of Antarctic sea ice predictability during ice-growth season (Holland et al., 2013; Marchi et al., 2019; Zunz et al., 2015). Our sea ice predictability results show the termination of both summer persistence and spring reemergence consistently occuring in July.

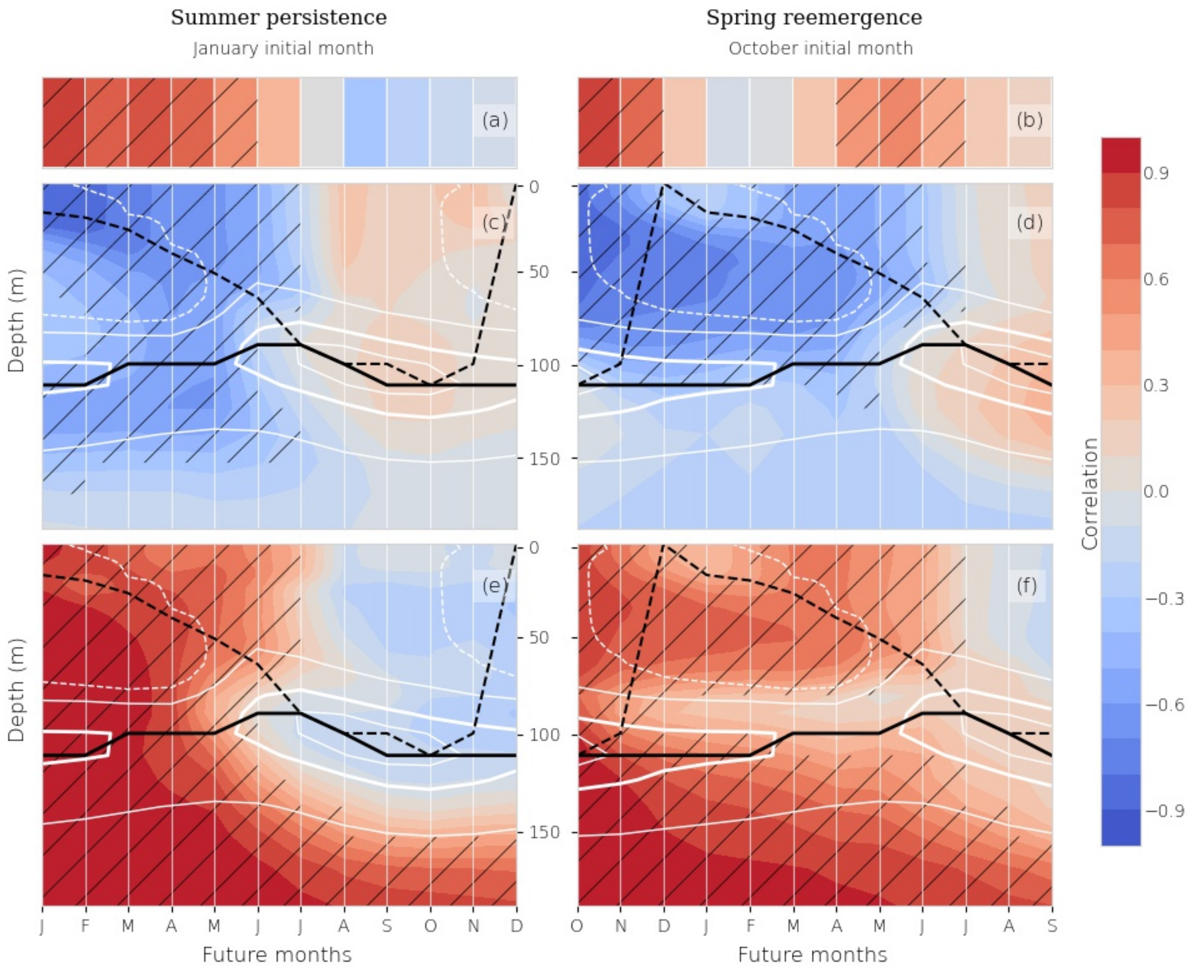

Figure 2: Comparison of summer persistence (plots on the left) and spring reemergence patterns (plots on the right) evident from sea ice (top row) and upper ocean predictability (0-200m) (middle and bottom row). Sea ice predictability: correlation of SIA from January (a) and October (b) initial months with future months; Correlation between SIA in (c) January and (d) October with ocean temperature in future months; Correlation of ocean temperature in (e) January and (f) October with future months. Statistically significant values (>95%) are hatched in all panels. In the oceanic predictability results (c-f), thick black line is the vertical temperature gradient (dT/dz) maximum, dashed black line is the vertical density gradient (dρ/dz) maximum, white contours are dT/dz contours, and white dashed contours bound the dT/dz values that are negative during summer stratification.

3.2 Ocean-ocean and ice-ocean correlations

The physical processes in the ocean underlying sea ice predictability patterns are investigated using the evolution of upper ocean predictability (Figure 2). We choose SIA correlations starting from January and October to represent summer persistence and spring reemergence patterns respectively (Figure 2 a and b). We correlate January and October SIA with lagged ocean temperature to explore how sea ice anomalies are related to upper ocean temperature (ice-ocean correlation) (Figure 2 c and d); the ocean's internal predictability is characterised by correlating the January and October temperature with future temperature at the same depth (ocean-ocean correlation) (Figure 2 e and f). We find a consistent evolution of predictability between the three sets of correlations. Sea ice and ocean autocorrelations (Figure 2 a,b, e, f), are positive, while ice-ocean correlations are negative, since cooler temperature implies more ice.

3.2.1 Seasonal evolution of the upper ocean

We overlay the climatological vertical thermal and density gradient contours to follow the seasonal evolution of the water column. The climatological dT/dz maximum (black line) represents the permanent pycnocline (PP) that separates the Winter Water (WW; i.e., cold water formed during sea ice production and its summer remnant) from slowly modifying Circumpolar Deep Water (CDW). The dρ/dz maximum (dashed black line) marks the evolution of seasonal pycnocline, which forms the base of the seasonally evolving mixed layer that is in direct exchange with the surface. Seasonal pycnocline acts as the base of mixed layer in summer (January-March) and autumn (April-June), before it merges with PP in winter.

During the ice growth season, the PP coincides with the maximum depth of statistically significant correlation (Figure 2d). There is a layer of weak correlations at the base of the WW (Figure 2f), which we interpret as noise, due to the high variability from mixing processes at the interface of the upper ocean and ocean interior. This separation (weak correlations) at the base of WW is expected, since WW is modified by sea ice production, implying that the entire WW is a source of memory for the ice-ocean system.

3.2.1 Freeze and melt as limits to predictability

The correlations emerging from October encounter loss of predictability during summer lag months, and present predictability remergence (Figure 2 b,d,f). Consistent with Holland et al. (2013) and Marchi et al. (2019), the oceanic predictability shows the weakening or loss of correlations during summer near the surface, while strong correlations are retained below this surface layer and above the PP. Freshwater and surface ocean warming during the ice-melt season (December-February) produce a thin and highly-stratified surface layer that becomes the summer mixed layer (dashed black line) in Figure 2c-f). This summer layer separates the thermal anomalies in the WW layer from the surface, causing the loss of predictability between December and March (Figure 2 b, d, f).

In March, the regime shifts from sea ice melt (and a well-stratified summer mixed layer) to sea ice production (and destratification at the surface). Brine rejection from sea ice growth induces vertical mixing, resulting in entrainment across the seasonal mixed layer. Initially, this entrainment reconnects relatively cold remnant WW layer with the surface layer, leading to the reeemergence of both sea ice and ocean predictability (Holland et al., 2013; Marchi et al., 2019). After entraining through the WW layer, the mixed layer continues to deepen, eventually reaching the PP (merging of dashed black line with black line in Figure 2 c-f). Further entrainment causes loss of predictability (Figure 1c and all panels of Figure 2) as it entrains water that has no sea ice process-related memory. We call this loss in predictability the ‘predictability barrier’, which is discussed in section (4.1).

3.2.2 Sensitivity of sea ice predictability to the stratification strength at the base of WW

The main distinction between ice-ocean correlations and ocean-ocean correlations is that ice-ocean correlations are largely bounded by the PP (upper 100 m), while the ocean-ocean correlations produce significant correlations below the PP (below 100m). As discussed in section 3.2.1, ice-ocean correlations emerging from October are bounded by the PP, which we attribute to the sea ice memory being confined to the WW. However the January SIA is correlated with ocean temperatures below the PP (up to 50 m; Figure 2c). Here we put forward the hypothesis that this is due to changes in the strength of the stratification at the base of the WW (or at the PP) (Figure 3e).

Winter cooling and sea ice production create a WW layer that is very distinct from CDW, which maintains a strong PP; therefore, the sea ice memory is confined above PP. When WW production ceases after October the pycnocline starts to decay allowing sea ice signals to penetrate deeper, so in January the ocean memory extends below the PP (Figure 2c). Ice-ocean correlations for all 12 initial months (Supplementary figure 1 (S1)) show how the correlations responds to changes in stratification strength. When stratification is strong at the PP (April-October), the PP act as the boundary for sea ice memory and ice-ocean correlations gradually extend below the PP when the stratification weakens at the PP (November-May, Figure S1). Doddridge et al. (2021) demonstrated that during the ice melt season, turbulent mixing can move heat anomalies downwards across the summer mixed layer and into the remnant WW layer; here we posit a similar process happening before the development of the summer mixed layer, so that temperature anomalies penetrate below the PP. In this case, the memory from those thermal anomalies is lost to the CDW (which acts as a thermal sink).

Importantly, this variability in the depth of significant correlation (Figure 2 c,d) demonstrates that the strength of stratification, as well as the depth, of the PP is important for the regime of sea ice predictability in a given sector. We further discuss the dependance-of sea ice predictability on the hydrographic profile in section 4.2.

4 Discussions

4.1 Predictability barrier and predictability suppression

Our study is consistent with findings from existing literature connecting upper OHC (oceanic thermal memory) with sea ice predictability (Holland et al., 2013; Marchi et al., 2019; Ordoñez et al., 2018; Zunz et al., 2015). In the Weddell Sea, sea ice anomalies persist in spring, are lost temporarily in summer (December-May), and then reemerges in May before they are lost permanently in mid-winter (July). Seasonal loss of sea ice predictability (in summer) is associated with the development of a highly stratified summer mixed layer due to sea ice melt that separates the surface ocean and sea ice from the heat content anomalies below the summer mixed layer. Below the summer mixed layer, OHC anomalies are retained and reemerge when the summer mixed layer erodes and deepen in autumn. This is consistent with the reemergence mechanism explained by Holland et al. (2013) and Marchi et al. (2019).

After reemerging, predictability is suddenly lost in mid-winter (in July). The loss in predictability is consistent among all three sets of correlation analysis. We call this loss in predictability the "predictability barrier". In our analysis, the predictability barrier is a clear, sharp loss of correlations in July (regardless of the lead month) and not the gradual decline we might expect from statistical red noise. This implies there is a change in the physical system in July. Previous studies (Blanchard-Wrigglesworth et al., 2011; Giesse et al., 2021; Ordoñez et al., 2018) also show the permanent loss of predictability on a specific month (or a set of months, in the same season) but they do not explain the physical mechanism of this barrier.

Since predictability arises from OHC in the mixed layer, loss of predictability suggests modification of OHC within mixed layer. Mixed layer can lose heat to the atmosphere and can gain heat from the ocean interior. The climatological sea ice freezing rate (Figure 3a), shows no sudden increase, suggesting there is no sudden changes in ocean-atmosphere fluxes that could explain a sudden loss of predictability. In section 3.2, we have shown the predictability barrier coincides with the time at which the seasonal pycnocline merges with PP. During the ice growth season, the atmosphere cools the upper ocean inducing sea ice growth, and deepening the mixed layer through enhanced vertical mixing from the brine released. Initially this entrains remnant WW containing sea ice memory into the mixed layer, which explains the reemergence of predictability. Once the mixed layer deepens to reach the PP, further sea ice growth entrains heat from ocean interior (CDW) into the mixed layer (Gordon and Huber, 1984; Gordon and Huber, 1990; Martinson, 1990; Wilson et al., 2019), which has no sea ice-related memory, therefore terminating predictability.

Martinson (1990) and Wilson et al. (2019) showed that vertical heat flux driven by brine rejection placed a constraint on winter sea ice growth. Our analysis shows that this constraint is likely invoked in mid-winter in the Weddell sector, when warm CDW is entrained into the mixed layer. The timing of predictability barrier signals when the negative ice-ocean feedback limiting ice growth rate due to entrainment is activated.

Goosse and Zunz (2014) and Lecomte et al. (2017) showed how increased stratification in the upper ocean reduced vertical heat flux from CDW during ice-growth, which enabled positive ice-ocean feedbacks. Lecomte et al. (2017) found the postive ice-ocean feedback, associated to a long term trend in sea ice concentration only in the Ross sector. The fact that they do not find positive ice-ocean feedback in the Weddell sea, is consistent with our finding of the existence of a predictability barrier that prevents the persistence of anomalies beyond 12 months. Therefore, an implication of predictability barrier is that it hampers near-surface ice-ocean feedbacks that could potentially lead to long term trends (in upper ocean properties and sea ice concentration).

By investigating regional Antarctic sea ice predictability one can determine the presence or absence of predictability barriers that will provide valuable insights into long term sea ice trends.

4.2 Dependence of sea ice predictability to mixed layer depth/ winter water depth

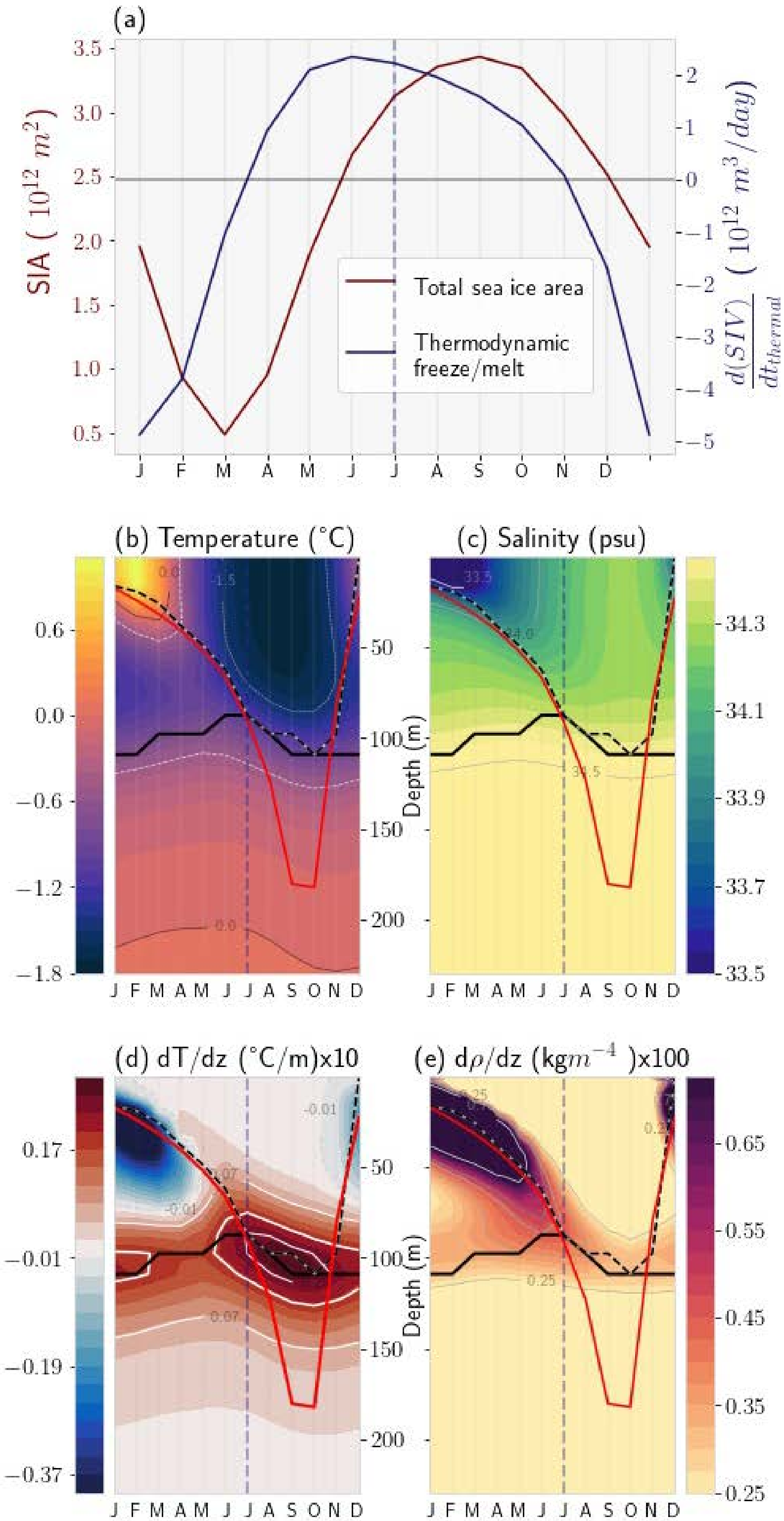

Figure 3: Annual evolution of climatological (a) Sea ice area (red line) and thermodynamic freeze and melt (blue line), (b) Temperature, (c) Salinity, (d) vertical temperature gradient (dT/dz), and (e) vertical density gradient (dρ/dz), spatially averaged over the sea ice covered ocean zone of the Weddell sector in the upper 250m. The vertical temperature gradient maximum (thick black line), vertical temperature gradient (white lines), and vertical density gradient maximum (dashed line) are the same used in Figure 2, and mixed layer depth (red line) is marked on all panels.

Mixed layer depth (MLD) has been given high relevance in previous studies of sea ice predictability. Holland et al. (2013) and Marchi et al. (2019) observed spatial variability in their prognostic sea ice predictability analysis, and suggested that sufficently deep mixed layers were required for retaining heat anomalies and hosting sea ice predictability. Our results align closely with findings from Marchi et al. (2019) in that the temperature anomalies relevant to sea ice predictability are stored at the depth range typical of WW. However as discussed in section 3.2.2, we find instances where the depth to which temperature anomalies extend, vary depending on the stratification strength at the PP. When the stratification is weak the T anomalies (memory) extends deeper than the WW. Also, Marchi et al. (2019) suggested that the effectiveness of the reemergence mechanism is associated with sufficiently large seasonal cycle of MLD (i.e., a transition from a shallow highly-stratified summer mixed layer to the deep WW). However, Ordoñez et al. (2018) suggested that variable mixed layer depth is less important to sea ice predictability than basic mixed layer temperature persistence, suggesting that the MLD is not the only important criterion for sea ice predictability during melt and growth season.

We have used the maximum vertical temperature gradient (dT/dz) to denote the PP and the base of the WW layer; We also used the maximum density gradient (dρ/dz) to follow the seasonal evolution of the mixed layer (more information in supporting information (TextS1, Figure S2)). From Figure 3b-e we can see how these two gradients compare with the model derived MLD. The MLD and dρ/dz maximum (red and dashed black line) closely align until July. However, during winter the MLD is considerably deeper than the dρ/dz maximum which is near PP. Our key finding is that sea ice and ocean predictability patterns follow changes in vertical ocean structure (dT/dz and dρ/dz gradients; Figure 2, all panels). Therefore, the vertical ocean structure in any region and its modification via sea ice processes, determines its potential for retaining oceanic thermal memory, and by focusing only on the mixed layer depth, we lose other key features and processes related to sea ice predictability and its spatial variability.

Our analysis looks at changes in total sea ice area and ocean properties averaged over a large area, in the Weddell Sea. We do not consider the variability within the region, such as the transport of sea ice into or out of the region, nor the advection of oceanic properties. Although the Weddell gyre forces a strong redistribution of sea ice within our sector, we estimate from the model that ~92% of the sea ice freezes and melts within our Weddell sector; hence in a bulk scale, the net dynamic term is minimal compared to thermodynamic freeze/melt. We rely solely on the correlations to draw our interpretations and use the climatological oceanic parameters to guide our arguments. Quantifying the seasonal exchanges and thermal modifications occurring in the upper ocean is a potential follow-up analysis.

5 Conclusions

Over the 40 years of satellite record of Antarctic sea ice, the last decade has seen particularly large fluctuations in sea ice extent, including a record high value in 2014, followed by a record low in 2016-17. These recent fluctuations and the uncertainties in sea ice variability and trends linked to climate change make the emerging field of sea ice prediction particularly relevant. In this study we have analyzed the predictability of sea ice and underlying ocean in the Weddell sector of the Southern Ocean, using lagged correlations. We find that 1) sea ice predictability emerging from summer months persists until mid-winter, and 2) sea ice predictability emerging from spring months has a temporary loss during summer months and reemerges in autumn months. We also find that oceanic predictability is largely confined to the Winter Water layer, and it is dependent not only on the depth of the Winter Water layer but also heavily controlled by changes in the strength of stratification at the base of the Winter Water layer. Therefore, both these hydrographic parameters may be valuable for understanding regional differences in Antarctic sea ice trends and variability.

Our results are consistent with Holland et al. (2013) and Marchi et al. (2019) in (1) connecting upper ocean heat content with sea ice predictability and (2) with their proposed mechanism of predictability reemergence. In addition to the temporary loss of predictability in summer lag months prior to predictability reemergence, we find a more permanent loss of predictability in mid-winter. In mid-winter when the seasonal pycnocline merges with the permanent pycnocline, warm Circumpolar Deep Water with no sea ice related memory entrains into the mixed layer and terminates the predictability. Key insights from our study are in finding that (1) regional sea ice predictability is tied to the vertical structure of its oceanic properties and how this structure evolves, especially when forced by sea ice processes. This implies that the spatial variability in sea ice predictability can now be addressed based on local upper ocean vertical structure and sea ice processes. We also find that (2) the strength of stratification at the base of the Winter Water layer is relevant in determining potential for sea ice predictability.

Oceanic predictability can be summed up as thermal anomalies lingering in the ice-ocean system at interannual timescales. These thermal anomalies generate sea ice predictability, which implies that sea ice predictability is a signature of local ice-ocean interaction mediated by residual thermal anomalies. Therefore, our analysis not only improves our knowledge and capacity for operational Antarctic sea ice forecast, but it presents a potential tool for evaluating the regional signature of ice-ocean interactions. The fact that sea ice predictability is strongly tied to the vertical structure of oceanic properties suggest that changes in the upper ocean in a warming climate are likely to alter Antarctic sea ice predictability patterns in the future.

Acknowledgements

This project received grant funding from the Australian Government as part of the Antarctic Science Collaboration Initiative program. The Australian Antarctic Program Partnership is led by the University of Tasmania, and includes the Australian Antarctic Division, CSIRO Oceans and Atmosphere, Geoscience Australia, the Bureau of Meteorology, the Tasmanian State Government and Australia's Integrated Marine Observing System. SL and AM acknowledge support from the Australian Research Council Center of Excellence for Climate Extremes (CE170100023). AM was supported by the Australian Research Council Discovery Early Career Research Award project DE200100414. SL acknowledges Quantitative Marine Science (QMS) research scholarship (including support from the CSIRO Postgraduate scheme), University of Tasmania tuition fee scholarship. This research was undertaken with the assistance of resources from the National Computational Infrastructure (NCI), which is supported by the Australian government.

We thank the Consortium for Ocean-Sea Ice Modelling in Australia (COSIMA; www.cosima.org.au), funded by the Australian Research Council through its Linkage Program (LP160100073), for making the ACCESS-OM2 suite of models available here https://doi.org/10.5281/zenodo.2653246 and here https://github.com/COSIMA/access-om2. All model outputs are open source, and the simulations presented in this manuscript is stored as part of the COSIMA data collection here: https://doi.org/10.4225/41/5a2dc8543105a. Passive microwave sea ice data are publicly available, hosted by the National Snow and Ice Data Center (https://nsidc.org/data/g02202/versions/3/).

References

Abernathey, R. P., Cerovecki, I., Holland, P. R., Newsom, E., Mazloff, M., & Talley, L. D. (2016). Water-mass transformation by sea ice in the upper branch of the Southern Ocean overturning. *Nature Geoscience, 9*, 596. doi:10.1038/ngeo2749
https://www.nature.com/articles/ngeo2749#supplementary-information

Blanchard-Wrigglesworth, E., Armour, K. C., Bitz, C. M., & DeWeaver, E. (2011). Persistence and Inherent Predictability of Arctic Sea Ice in a GCM Ensemble and Observations. *Journal of Climate, 24*(1), 231-250. doi:10.1175/2010jcli3775.1

Brandt, R. E., Warren, S. G., Worby, A. P., & Grenfell, T. C. (2005). Surface albedo of the Antarctic sea ice zone. *Journal of Climate, 18*(17), 3606-3622.

Bushuk, M., Winton, M., Haumann, F. A., Delworth, T., Lu, F., Zhang, Y., . . . Zeng, F. (2021). Seasonal prediction and predictability of regional Antarctic sea ice. *Journal of Climate*, 1-68. doi:10.1175/jcli-d-20-0965.1

Chen, D., & Yuan, X. (2004). A Markov Model for Seasonal Forecast of Antarctic Sea Ice. *Journal of Climate, 17*(16), 3156-3168. doi:10.1175/1520-0442(2004)017<3156:Ammfsf>2.0.Co;2

Doddridge, E. W., Marshall, J., Song, H., Campin, J.-M., & Kelley, M. (2021). Southern Ocean Heat Storage, Reemergence, and Winter Sea Ice Decline Induced by Summertime Winds. *Journal of Climate, 34*(4), 1403-1415. doi:10.1175/jcli-d-20-0322.1

Giesse, C., Notz, D., & Baehr, J. (2021). On the Origin of Discrepancies Between Observed and Simulated Memory of Arctic Sea Ice. *Geophysical Research Letters, 48*(11), e2020GL091784. doi:https://doi.org/10.1029/2020GL091784

Goosse, H., & Zunz, V. (2014). Decadal trends in the Antarctic sea ice extent ultimately controlled by ice–ocean feedback. *The Cryosphere*(2), 453. doi:10.5194/tc-8-453-2014

Gordon, A. L., & Huber, B. A. (1984). Thermohaline stratification below the Southern Ocean sea ice. *Journal of Geophysical Research: Oceans, 89*(C1), 641-648.

Gordon, A. L., & Huber, B. A. (1990). Southern ocean winter mixed layer. *Journal of Geophysical Research, 95*(C7), 11655. doi:10.1029/jc095ic07p11655

Guemas, V., Chevallier, M., Déqué, M., Bellprat, O., & Doblas-Reyes, F. (2016). Impact of sea ice initialization on sea ice and atmosphere prediction skill on seasonal timescales. *Geophysical Research Letters, 43*(8), 3889-3896.

Handcock, M. S., & Raphael, M. N. (2020). Modeling the annual cycle of daily Antarctic sea ice extent. *The Cryosphere, 14*(7), 2159-2172. doi:10.5194/tc-14-2159-2020

Hobbs, W. R., Massom, R., Stammerjohn, S., Reid, P., Williams, G., & Meier, W. (2016). A review of recent changes in Southern Ocean sea ice, their drivers and forcings. *Global and Planetary Change, 143*, 228-250. doi:https://doi.org/10.1016/j.gloplacha.2016.06.008

Holland, M. M., Blanchard-Wrigglesworth, E., Kay, J., & Vavrus, S. (2013). Initial-value predictability of Antarctic sea ice in the Community Climate System Model 3. *Geophysical Research Letters, 40*(10), 2121-2124. doi:10.1002/grl.50410

Holland, P. R. (2014). The seasonality of Antarctic sea ice trends. *Geophysical Research Letters, 41*(12), 4230-4237. doi:10.1002/2014gl060172

Juricke, S., Goessling, H. F., & Jung, T. (2014). Potential sea ice predictability and the role of stochastic sea ice strength perturbations. *Geophysical Research Letters, 41*(23), 8396-8403.

Kearney, K. A., Alexander, M., Aydin, K., Cheng, W., Hermann, A. J., Hervieux, G., & Ortiz, I. (2021). Seasonal Predictability of Sea Ice and Bottom Temperature Across the Eastern Bering Sea Shelf. *Journal of Geophysical Research: Oceans, 126*(11), e2021JC017545. doi:https://doi.org/10.1029/2021JC017545

Kiss, A. E., Hogg, A. M., Hannah, N., Boeira Dias, F., Brassington, G. B., Chamberlain, M. A., . . . Duran, E. R. (2020). ACCESS-OM2 v1. 0: a global ocean-sea ice model at three resolutions. *Geoscientific Model Development, 13*(2), 401-442.

Lecomte, O., Goosse, H., Fichefet, T., Barthélemy, A., De Lavergne, C., & Zunz, V. (2017). Vertical ocean heat redistribution sustaining sea-ice concentration trends in the Ross Sea. *Nature Communications, 8*(1). doi:10.1038/s41467-017-00347-4

Marchi, S., Fichefet, T., & Goosse, H. (2020). Respective influences of perturbed atmospheric and ocean–sea ice initial conditions on the skill of seasonal Antarctic sea ice predictions: A study with NEMO3.6–LIM3. *Ocean Modelling*, *148*, 101591. doi:https://doi.org/10.1016/j.ocemod.2020.101591

Marchi, S., Fichefet, T., Goosse, H., Zunz, V., Tietsche, S., Day, J. J., & Hawkins, E. (2019). Reemergence of Antarctic sea ice predictability and its link to deep ocean mixing in global climate models. *Climate Dynamics*, *52*(5), 2775-2797. doi:10.1007/s00382-018-4292-2

Martinson, D. G. (1990). Evolution of the southern ocean winter mixed layer and sea ice: Open ocean deepwater formation and ventilation. *Journal of Geophysical Research: Oceans*, *95*(C7), 11641-11654. doi:10.1029/JC095iC07p11641

Massom, R. A., & Stammerjohn, S. E. (2010). Antarctic sea ice change and variability – Physical and ecological implications. *Polar Science*, *4*(2), 149-186. doi:https://doi.org/10.1016/j.polar.2010.05.001

Massonnet, F., Reid, P., Lieser, J., Bitz, C., Fyfe, J., & Hobbs, W. (2019). Assessment of summer 2018-2019 sea-ice forecasts for the Southern Ocean.

Meier, W. N., Fetterer, F., Savoie, M., Mallory, S., Duerr, R., & Stroeve, J. (2013). *NOAA/NSIDC Climate Data Record of Passive Microwave Sea Ice Concentration*. Retrieved from: https://nsidc.org/data/docs/noaa/g02202_ice_conc_cdr/

Ordoñez, A. C., Bitz, C. M., & Blanchard-Wrigglesworth, E. (2018). Processes Controlling Arctic and Antarctic Sea Ice Predictability in the Community Earth System Model. *Journal of Climate*, *31*(23), 9771-9786. doi:10.1175/jcli-d-18-0348.1

Raphael, M. N., & Hobbs, W. (2014). The influence of the large-scale atmospheric circulation on Antarctic sea ice during ice advance and retreat seasons. *Geophysical Research Letters*, *41*(14), 5037-5045. doi:10.1002/2014gl060365

Tsujino, H., Urakawa, S., Nakano, H., Small, R. J., Kim, W. M., Yeager, S. G., . . . Bentsen, M. (2018). JRA-55 based surface dataset for driving ocean–sea-ice models (JRA55-do). *Ocean Modelling*, *130*, 79-139.

Wilson, E. A., Riser, S. C., Campbell, E. C., & Wong, A. P. S. (2019). Winter Upper-Ocean Stability and Ice–Ocean Feedbacks in the Sea Ice–Covered Southern Ocean. *Journal of Physical Oceanography*, *49*(4), 1099-1117. doi:10.1175/jpo-d-18-0184.1

Yang, C.-Y., Liu, J., Hu, Y., Horton, R. M., Chen, L., & Cheng, X. (2016). Assessment of Arctic and Antarctic sea ice predictability in CMIP5 decadal hindcasts. *The Cryosphere*, *10*(5), 2429-2452. doi:10.5194/tc-10-2429-2016

Zampieri, L., Goessling, H. F., & Jung, T. (2019). Predictability of Antarctic Sea Ice Edge on Subseasonal Time Scales. *Geophysical Research Letters*, *46*(16), 9719-9727. doi:10.1029/2019gl084096

Zunz, V., Goosse, H., & Dubinkina, S. (2015). Impact of the initialisation on the predictability of the Southern Ocean sea ice at interannual to multi-decadal timescales. *Climate Dynamics*, *44*(7-8), 2267-2286.